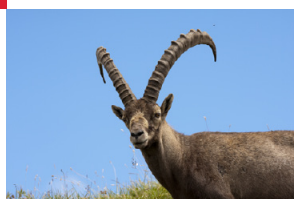

Abstract Volume
9th Swiss Geoscience Meeting

Zurich, 11th – 13th November 2011

18. Advances in GIScience and Remote Sensing

sc | nat

Geosciences
Platform of the Swiss Academy of Sciences

ETH
Eidgenössische Technische Hochschule Zürich
Swiss Federal Institute of Technology Zurich

18. Advances in GIScience and Remote Sensing

Michael Schaepman, Robert Weibel, Ross Purves, Markus Rothacher, Konrad Schindler

Swiss Commission for Remote Sensing,
Interuniversitäre Partnerschaft für Erdbeobachtung und Geoinformatik (IPEG)

TALKS:

18.1 *Breschan J., Heinimann H. R., Niederhuber M.:* Automatic identification of forest treatment units using LiDAR-data

18.2 *Demir N., Baltsavias E.:* Automated modelling of 3D building roofs using LIDAR and image data

18.3 *Derungs C., Purves R.:* Identifying and disambiguating toponyms

18.4 *Henke D., Meier E.:* Initial results of a low-frequency 3D-SAR approach for mapping glacier volumes

18.5 *Leinß S., Hajnsek I.:* Sensitivity of X-band SAR interferometry on the snow pack characterisation

18.6 *Waser, L.T., Ginzler, C, and Kuechler, M.:* Large-Area Tree Species Classification – Potential And Limits Of Airborne Digital Sensor (Ads40/80) Data For The Swiss Nfi

POSTERS:

P 18.1 *D'Odorico P., Hueni A., Jehle M., Schaepman M.:* Recent efforts on APEX Calibration and Validation

P 18.2 *de Jong R., Verbesselt J., Schaepman M.E., de Bruin S.:* Short-term variability within long-term trends in global vegetation activity

P 18.3 *Saurer O., Baatz G., Köser K., Pollefeys M.:* Visual Localization Recognition and Photo-to-Terrain-Alignment in Mountainous Areas

P 18.4 *Schubert A., Small D., Jehle M., Meier E.:* Long-term geolocation accuracy of TerraSAR-X high-resolution spotlight products

P 18.5 *Torabzadeh H., Morsdorf F., Schaepman M.:* Data fusion methods of LiDAR and spectroscopy data for the derivation of forest biochemical and biophysical variables – a review

P 18.6 *Weyermann J., Damm A., Kneubühler M., Schaepman M.:* Ross-Li BRDF correction of airborne imaging spectroscopy data for improved continuous field map generation in the Swiss National Park

P 18.7 *Yáñez-Rausell L., Malenovsky Z., Schaepman M.:* Influence of gap fraction on coniferous needle optical properties measurements

P 18.8 *V.L. Muldera, S. de Bruin, M.E. Schaepman:* Towards spectroscopic modelling of composite mineralogy

18.1

Automatic identification of forest treatment units using LiDAR-data

Breschan Jochen[1], Heinimann Hans Rudolf[1] & Niederhuber Monika[1]

[1]*Institut für Terrestrische Ökosysteme ITES, ETH Zürich, CHN K73.1, CH-8092 Zürich (jochen.breschan@env.ethz.ch)*

The management of forests requires the delineation of treatment units. Forest stands traditionally serve as treatment units. They are characterized by their stage-of-development (SoD). The SoD is classified into the six categories that represent ranges of the median diameter-at-breast-height (DBH) of the tallest trees within a forest stand (Schütz 2003). In the past, this delineation process was carried out by hand, i.e., using stand information gained from terrestrial inventories. However, the application of such an approach has become too expensive in the recent decades.

Here, we present an automated method of stand delineation that uses a spatially explicit forest inventory computed from high resolution LiDAR (Light Detecting And Ranging) surface- and terrain data. It is captured as a flow chart in Figure 1, that is structured into a forest inventory- and a stand delineation module.

The forest inventory module starts with the extraction of single trees on a Canopy Height Model (CHM, cell size 0.5 m) that was previously computed from the digital surface- and terrain model (DSM, DTM). Tree extraction algorithms have been widely studied in the recent decade (e.g., Kaartinen (2008) gives an overview on the performance of nine extraction methods). Here, we employ an algorithm inspired by Hyyppae (2001) that locates single trees at the local maxima of a filtered CHM. The biometric key figures, tree height and tree diameter, are then estimated based on the CHM.

The stand delineation module generalizes the forest inventory information, aiming to identify homogenous forest stands (i.e., aggregation of adjacent trees having a similar DBH). A fuzzy inference system first assigns the SoD to each tree based on its biometric key figures. This includes a DBH estimation as a function of tree height and crown diameter, using transfer functions (Ye 1995). The stand delineation is then processed based on the resulting "SoD-per-tree" raster by using a filter -method. It identifies the SoD with respect to the tallest trees (according their SoD-category) within the filter window for each cell on the grid raster.

This model has been implemented in Matlab, and was carried out on a coniferous forest in the Canton of Grisons. First results indicate that the method plausibly classifies the single trees according to the SoD. Stand delineation using the filter method retrieves plausible forest stands for filter windows ≥800m^2. However, the perimeters of the single stands are zig-zag shaped and require more generalization to serve as operational treatment units. We are currently working on a clustering-approach that may overcome the shortcoming of the filter-method.

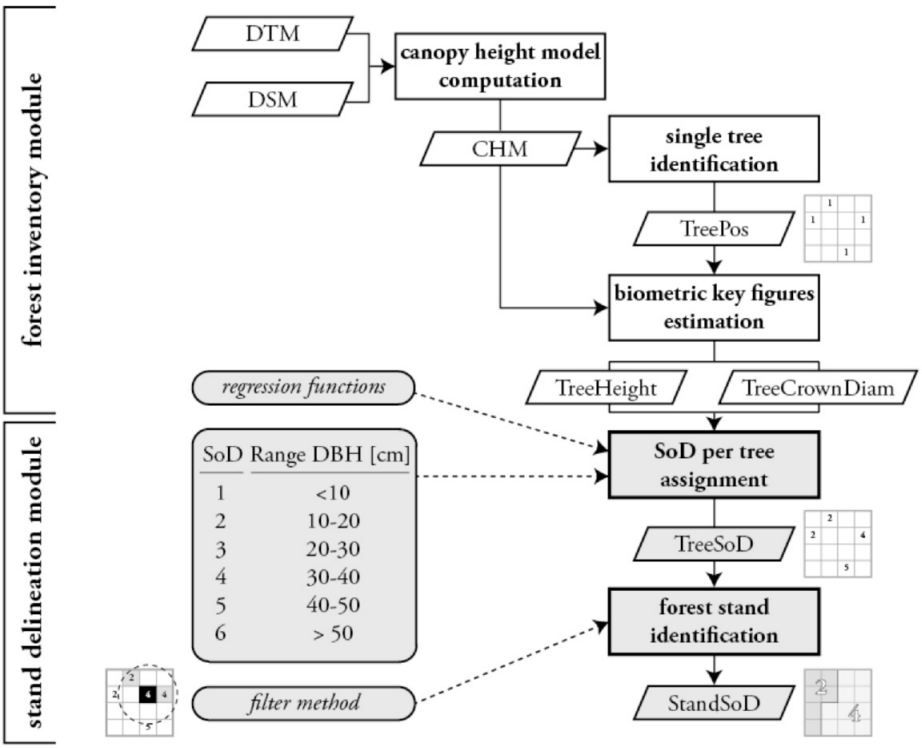

Figure 1. Model conceptualization of the automatic stand delineation method, consisting of a forest inventory- and a stand delineation module. The former module extracts single trees on a CHM raster grid and assigns biometric key figures. The latter module classifies each tree into its corresponding stage-of-development (SoD), and then aggregates the single trees into forest stands using a filter-method.

REFERENCES

Hyyppae, J., et al. 2001. A segmentation-based method to retrieve stem volume estimates from 3-d tree height models produced by laser scanners, IEEE Transactions on Geoscience and Remote Sensing, 39, 969– 975.

Kaartinen, H., et al. 2008: Accuracy of automatic tree extraction using airborne laser scanner data, Proceedings of SilviLaser 2008: 8th international conference on LiDAR applications in forest assessment and inventory, 467-476.

Morsdorf, F., et al. 2004: LIDAR-based geometric reconstruction of boreal type forest stands at single tree level for forest and wildland fire management, Remote Sensing of Environment, 92, 353-362.

Schütz, J.-P. 2003 : Waldbau I – Die Prinzipien der Waldnutzung und der Waldbehandlung, http://www.wm.ethz.ch/docs/document/fm1.

Ye, R. 1995: Waldsimulation auf der Basis automatischer Luftbildmessung und unter Kontrolle von GIS, Mitteilungen der Abteilung für Forstliche Biometrie 95-1, Freiburg i. Brsg.

18.2

Automated modelling of 3D building roofs using LIDAR and image data

Demir Nusret[1], Baltsavias Emmanuel[1]

[1] *Institute of Geodesy and Photogrammetry, ETH Zurich, 8093,Switzerland (demir,manos@geod.baug.ethz.ch)*

In this work, an automated approach has been developed for 3D roof modeling. The method consists of two main parts; the first one is the detection and the second is modeling of the roofs. A raw LIDAR point cloud with 5pts/1sqm resolution and DMC digital camera images with 8 cm GSD have been used for testing the developed methods.

For the detection of buildings, four different approaches are used and combined for achieving the best detection result. In the first approach, a slope-based morphological filter is used to detect all off-terrain objects (which include buildings, trees and other objects) using a DSM from image matching. After that, the trees are eliminated by unsupervised classification of the NDVI image. The second approach is based on a multispectral classification refined with height information from LIDAR data. In the third approach, above-terrain objects are detected from LIDAR data and the vegetation is eliminated using NDVI classification. The last approach is based on the detection and elimination of the trees using the vertical density of the raw LIDAR data. The results from the four alternative approaches are combined with Boolean operations in accordance with their advantages. The correctness of the detection has been calculated as 90% with 17% omission error. The detected regions are enlarged a bit to include, if possible, all points which belong to the roofs.

For the modeling part, the process chain starts with detection of planar features using the RANSAC approach using the LIDAR data in the previously detected building regions. Since the plane detection is a parameter sensitive approach, the detected planes are refined according to the neighborhood of the LIDAR points. During the refinement process, the distance of every point has been calculated to the assigned plane of the neighboring point. If the distance is in a certain threshold, (in our case it has been set as 0.2 m, the accuracy of LIDAR points), the plane assignment of the point has been changed to the plane of the neighboring point if its size is bigger than the actual plane size. After this refinement process, region growing is applied to split the over-segmented planes. In the next step, the planes are classified as wall, terrain and roof planes based on their slope and their relative height from the terrain surface. Existing neighboring tree points are eliminated by vertical density analysis. After that, only the roof points are used for the modeling approach.The alpha shape algorithm is used in the reconstruction of the roof outlines.

3D line segments from edge matching of stereo images are used to increase the positional accuracy and to eliminate the irregularity of the outlines. To generate 3D line segments, 2D line segments are extracted and matched across multiple images (Ok et. al. 2009). Additionally, the intersection edges are extracted from the intersection of the roof surfaces. 3D lines are assigned to the plane surfaces whenever they fit them within a certain distance threshold. Then the neighboring LIDAR points to 3D lines are eliminated and the alpha shape algorithm is applied again to generate the roof outlines. Since the 3D lines can not be fully extracted for all buildings, the final regularization of the roof polygons are needed.

For this regularization, the RANSAC approach is used to fit the roof outlines to the straight lines and all fitted lines are intersected between each other. The intersection points which are closest to the first generated roof outlines are selected as roof corner points. The consecutive points are converted to the line features, if their turning angle is not an acute angle. Then, LIDAR points which are neighbors to the generated line features are deleted and the line features are added into the set of LIDAR points. The alpha shape algorithm is applied again and final 3D roof models are generated.

3D reference data is measured manually using DMC images. It is used for assessing the accuracy of the generated roof models. A set of criteria are considered for the comparison of the models. The first criterion is defined as the area of intersection of the models in union of the models. The second criterion is called as correctness, and is obtained by finding the intersection area of the models in the modeled roof model. The third one is called completeness. It is the area of the intersection of the models in the reference roof model. The fourth criterion is the average absolute distance, and the last one is the shifts in x,y,z between the models. The pairs for the comparison between the generated roof models and the reference models are defined according to the maximum value of the first criterion.

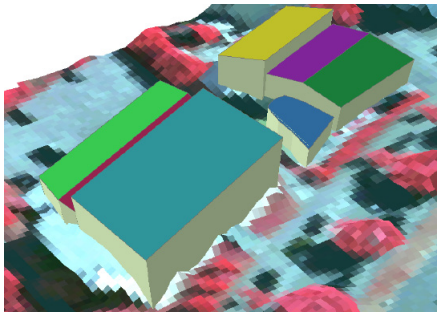

Figure 1. Some examples from the generated roof models

REFERENCES

Demir, N., & Baltsavias., E., 2010. Use of image and laser scanning data for building detection., in APRS, Vol. 38, Part 4,, Orlando, USA, 7 pp., on CD.

Ok, A.O., & Wegner, J.D., & Heipke, C., & Rottensteiner, F., & Soergel, U., &Toprak, V.:2010. A new straight line reconstruction methodology from multi-spectral stereo aerial images, in IAPRS vol. 38, part 3A, Paris, pp. 25-30

18.3

Identifying and disambiguating toponyms

Curdin Derungs and Ross Purves

Department of Geography, University of Zurich, Winterthurerstrasse 190, CH-8057

Toponyms are place names or named spatial entities. We are all familiar with them through their use on topographic maps and in everyday language. A statement such as: “Ich bin beim Dynamo am baden” is a typical example of the use of toponyms. They are the most natural way that people explicitly refer to locations in space, and allow us to deal well with ambiguity and uncertainty. They are not only found in speech, but also in written text and thus recognition of toponyms in documents is a key way of linking written language to explicit coordinates through the use of lists of toponyms and their associated geographic coordinates.

A number of disciplines, including Natural Language Processing and Geographic Retrieval are concerned with the question of correctly identifying toponyms in text. For instance, in the example given above we must distinguish between a *Dynamo* used to power our bike lights and *Dynamo*, the restaurant on the Limmat. In this example the things that we explicitly know about ‘Dynamo’, together with the context of the sentence, help us find an adequate answer. Another hint for could be a vague understanding of where, geographically speaking, ‘Ich’ is assumed to be and that the place ‘Dynamo’ is likely to be visited by this person to go swimming. In a nutshell: to solve this problem in an everyday sense we use both the text and contextual knowledge we have about the place and the activity being described.

To date, most methods addressing identification of toponyms have used relatively simple methods, such as population or position in administrative hierarchies to distinguish between different instances of the same toponym (so called geo-geo ambiguity – are we referring to London, England or London, Canada) and other contextual information to distinguish between geo-non geo ambiguity (am I in the bath or going to the city of Bath near Bristol)?

Spatial granularity (does the toponym describe a rock in the Engadine or a city) has received limited attention. However, if we wish to correctly resolve toponyms, it is clear that we must consider whether a document describes the history of the last bear to be shot in Val Mingèr or a journey from Basel to Luzern. Val Mingèr and the surrounding alps, forest and mountains are unknown to most people, even in a small country like Switzerland. We do not know a lot about all these places and little explicit knowledge can be found in accessible data sources about candidate toponyms. By contrast, for a journey between Basel and Zürich we have much more knowledge about not only these cities, but what is found on the journey and this information can be used when deciding if Zürich or Basel are toponyms and if so which locations they are likely to refer to.

Within our work we try to address the issue of missing toponym knowledge by using other, mostly geographic, sources. The basic assumption is that toponyms that co-occur in a document have something in common. The more closely they co-occur the greater the similarity. Previous work has shown that geographic proximity (Euclidean distance) is one such measurement. Alternatively, we might search for a toponym using a search engine and use the number of responses as a basic measure of common a toponym is. This already is a very helpful piece of information as we can assume that the toponyms used in a document follow some predictable patterns, rather than being random (e.g. one fixed level of famousness, like Zürich, Basel, Bern or a constant zoom from famous to unknown toponyms, e.g. Dynamo in Zürich). One example of a more geographic and novel type of context that we can add to toponyms takes the form of geomorphometric scope. Here we explore the geomorphometry of candidate toponyms, again with the expectation that similar toponyms might be found in similar settings (e.g. the cities of Zürich and Basel in predominately flat areas, and locations around Val Mingèr in steeper, more rough terrain). In our talk we will illustrate how the combination of such knowledge can be used in the resolution of toponyms, and help to disambiguate between toponyms particularly for fine-grained cases where other knowledge such as population or web prominence is not available.

18.4

Initial results of a low-frequency 3D-SAR approach for mapping glacier volumes

Daniel Henke, Meier Erich

Remote Sensing Laboratories (RSL), University of Zurich, Winterthurer Strasse 190, CH-8057 Zurich, Email: daniel.henke@geo.uzh.ch

In the context of natural hazard prevention and water management, climate change and sea level predictions (Solomon, 2007), the retention of water in glaciers is a key factor. In traditional approaches, the ice thickness of glaciers is either roughly approximated by extrapolating field measurements (drilling or Ground Penetrating Radar) or by a set of empirical or physically based relationships as e.g. mass conservation and principles of ice flow dynamics (Farinotti, 2009). In recent years, remote sensing in general and SAR specifically (Prats, 2007) contributes to precise large-scale measurements of glacier parameters. However, these methods are all restricted to the top layer of the glacier and information about its volume can only be derived indirectly from methods described above. In this paper, we present preliminary results of a 3D-SAR processing approach using low-frequency radar waves capable of penetrating the glacier ice up to a certain depth. 3D-SAR in other applications has been shown to provide accurate height estimates using techniques ranging from interferometry and cross correlation in circular tracks (Oriot, 2008) to tomographic processing of dual-pol data (Frey, 2008). However, the data for this study come from a campaign with a low-frequency SAR system (i.e. CARABAS sensor operating at center frequency of ~50 MHz) in 2003 over the Aletsch Glacier area, Switzerland, and were originally not acquired for 3D applications. Based on only these few, arbitrary flight tracks a method to calculate the height of the maximal backscattering response in the glacier ice and to approximate its volume was developed demonstrating the potential of SAR for mapping glacier volumes.

To generate a 3D estimate of the glacier bed, first a 3D reconstruction grid matrix is initialized with the Digital Elevation Model (DEM) values at the top layer in z-direction. Then for each flight track a 3D time-domain back-projection algorithm calculates for each voxel an intensity value as a standard 2D back-projection algorithm (Frey, 2008) does it for each pixel. We introduce an additional processing step to account for the refractivity of the glacier ice. Consequently, at each radar pulse of the flight track the points of entry at the glacier surface have to be determined. We make use of the spatial and temporal interrelationship between adjusted pixels to achieve computational efficiency. The absolute values of the result-

ing 3D-matrices for each flight track are multiplied to incoherently merge the single track results to one voxel image. For the common and generally more precise coherent adding the number of tracks and the orientation of the flight pattern are not appropriate. The maximal value in each z-column of the final, merged matrix corresponds to the maximum backscattering response of the radar signal and thus indicates the height of a potential glacier bed. Finally, we apply a low-pass filter to suppress noise effects and get a smooth, more realistic estimate of the surface.

This method was applied to a 5x5 km2 test site over the Konkordiaplatz with a horizontal resolution of 5m and a vertical resolution of 15m. Results are illustrated in Fig. 1. While for the snow and ice free surface (e.g. mountain tops) the highest backscattering response can be found in the top layers, in the glacier ice the low-frequency radar waves penetrate into the ice. It still has to be investigated whether the backscattering maxima is indeed caused by the bedrock or by other factors like a significant amount of moraine material, an unfavorable combination of crevasses, processing artifacts or poor signal-to-noise ratio.

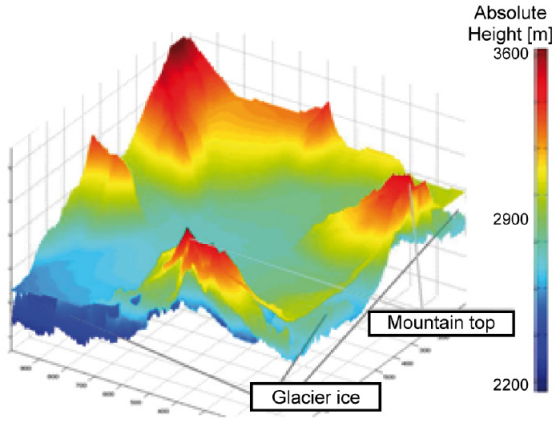

Fig. 1: DEM and 3D-SAR surface maps.

The results demonstrate the capability of low-frequency SAR sensors to potentially map glacier volumes in a large scale. Further campaigns with a flight track pattern optimized for the problem of 3D glacier mapping, and more research including ground truth validation, has to be done to verify the results. These ground truth validations are especially relevant to the question of how accurate the estimated height of the maximal backscattering is and how it is influenced by simplified physical assumptions and estimated processing parameters.

REFERENCES

Farinotti D., M. Huss, A. Bauder, and M. Funk (2009), "An estimate of the glacier ice volume in the Swiss Alps," *Global and Planetary Change*, vol. 68, pp. 225-231.

Frey O. and E. Meier (2008), "Tomographic Focusing by Combining Time-Domain Back-Projection and Multi-Looking Based Focusing Techniques," *European Conference on Synthetic Aperture Radar*, Friedrichshafen, Germany, vol. 2, pp. 73-75.

Oriot H. and H. Cantalloube (2008), "Circular SAR imagery for urban remote sensing," *European Conference on Synthetic Aperture Radar*, Friedrichshafen, Germany, vol. 2, pp. 205-208.

Prats, P., C. Andres, R. Scheiber, K. Macedo, J. Fischer and A. Reigber (2007), "Glacier Displacement Field Estimation Using Airborne SAR Interferometry," *IEEE Geoscience and Remote Sensing Symposium*, Barcelona, Spain, pp.2098-2101.

Solomon, S., D. Qin, M. Manning, Z. Chen, M. Marquis, K.B. Averyt, M. Tignor and H.L. Miller (eds.) (2007), *Contribution of Working Group I to the Fourth Assessment Report of the Intergovernmental Panel on Climate Change, 2007*, Cambridge University Press, Cambridge, United Kingdom and New York.

18.5

Sensitivity of X-band SAR interferometry on the snow pack characterisation

Leinß Silvan[1], Hajnsek Irena[1,2]

[1] *Institute of Environmental Engineering, ETH Zürich, Switzerland*
[2] *Microwaves and Radar Institute, German Aerospace Center (DLR), Germany*

The knowledge of the amount of snow cover and it's structure is an important parameter for freshwater reservoirs, flood prediction, hydroelectric power plants as well as weather, climate, and avalanche models [Barnett, 2005]. Still, the precise knowledge of snow properties relies on local and work-intensive ground measurements which are of limited value due to the high spatial variability of the snow cover. Investigating the optical regime provide high spatial resolution but depends on clear weather conditions and provides only snow surface information while passive microwave systems suffering from the very low spatial resolution (km-scale).

Within the last few years the development in SAR technologies allows image resolution on the meter-scale from space while the microwave frequencies penetrate the snow cover. The obtained data are able to provide parameters for snow pack characterisation. Among a series of important snow parameter are the snow volume, snow water equivalent (SWE) and structural properties. The satellite mission TerraSAR-X equipped with a synthetic aperture radar (SAR) system operating at the X-band frequency of 9,65 GHz provides dual polarimetric radar scenes with a resolution of 3.5 m, which allow multi-pass interferometric acquisitions with a time resolution of 11 days [Werninghaus, 2010]. Exploiting the complex phase of high resolution interferograms of different polarisations gives access to snow cover related parameters [Deep, 2011].

Volume scattering in the snow layer causes decorrelation of the complex coherence of two consecutive images. A simple two layer volume model is adapted that relates the complex interferometric coherence of the volume scattering directly to physical parameters as volume height, volume media extinction, underlying topography and the ground-to-volume ratio. A first analysis of snow property extraction by using time series data of interferometric TerraSAR-X data available over three different snow test sites is performed.

REFERENCES

Barnett, T. et al. D. 2005: Potential impacts of a warming climate on water availability in snow-dominated regions. Nature 438, 303-309.

Werninghaus, R & Buckreuss, S. 2010: The TerraSAR-X Mission and System Design. IEEE Transactions on Geoscience and Remote Sensing 48 (2), 606-614.

Deeb, E. et al. D. 2011: Monitoring snowpack evolution using interferometric synthetic aperture radar on the North Slope of Alaska. International Journal of Remote Sensing 32 (14), 3985-4003.

18.6

Large-area tree species classification – potential and limits of airborne digital sensor (ADS40/80) data for the Swiss NFI

Waser Lars[1], Ginzler Christian[1] & Kuechler Meinrad[2]

[1] *WSL, Landscape Dynamics, Swiss Federal Research Institute WSL, 8903 Birmensdorf, Switzerland – phone: +4144 7392292; email: waser(ginzler, kuechler)@wsl.ch*
[2] *WSL, Biodiversity and Conservation Biology*

Temporally frequent, cost-efficient and precise forest information requirements for NFIs, monitoring or protection tasks have grown over time and will continue to do so in the future. In Switzerland, the airborne digital sensors ADS40/ADS80 offers new opportunities as they can provide entire image strips with high geometric, radiometric and temporal resolution and cover the entire country every three years. This study presents an approach to semi-automated tree species classification on regional / state level for different types of forests using multispectral ADS40/ADS80 data to support some tasks of the Swiss National Forest Inventory (NFI).

Until now, most (semi)-automated species classification methods have been developed for small study areas of a few hectares with few field plots and for relatively homogeneous forests with only a few tree species. In the present study a robust model has been developed for an area located in the East of Switzerland with an extend of approx. 2500 km^2. The dominating deciduous tree species are *Fagus sylvatica* and *Fraxinus excelsior* and less frequently *Acer sp., Alnus sp.,* and *Betula sp.* The main coniferous trees are *Abies alba*, *Larix deciduas, Picea abie,* and *Pinus sylvestris*.

Ground surveys were carried out in summer 2009 and 2010, focusing on the most frequent tree species (at least 5% coverage in Switzerland). ADS80-SH82 and ADS40-SH52 RGB and CIR images with a spatial resolution of 0.25-0.5 m were used. Additionally, canopy height models (CHMs) were generated automatically from the images and from additional LiDAR terrain data with a spatial resolution of 0.5m. Prior to the object-oriented tree species classification, homogenous image segments of individual tree crowns and tree groups were obtained using a multi-resolution segmentation procedure.

In a second step, several variables (geometric and spectral signatures) were derived from the remote sensing data using standard digital image processing methods (including colour transformation, principal components analysis, arithmetic combinations). To obtain good predictions, a small set of powerful variables has to be selected using a stepwise variable selection (AIC, both-directions). The final input variables used in this study consist of original image bands, IHS and their PCAs. As the response variable has more than two possible states, multinomial regression models had to be applied.

To determine the predictive power of the models, a 10-fold cross-validation was applied. The overall accuracies vary between 0.65 and 0.85, and Cohen's kappa values between 0.55 and 0.75. Lower accuracies (kappa < 0.5) were obtained for small samples of species such as non-dominant (mostly deciduous) tree species with similar spectral properties. Currently, NFI sample plots are being implemented for validation.

Further development is needed with the harmonization of the several image strips recording trees with a different phenological status. For this, radiometric correction between images stripes will be taken into account.

For the Swiss NFI, the tree species composition of larger areas, preferably on the national scale is required, the findings of this preliminary study provide a first important contribution. Furthermore, the continuity of this approach will be guaranteed since the required input data (field samples, images) is being provided every three years by other national campaigns or monitoring programs.

REFERENCES

Waser, L.T., Küchler, M., Ecker, K., Schwarz, M., Ivits, E., Stofer, S., & Scheidegger, C. (2007). Prediction of Lichen Diversity in an Unesco Biosphere Reserve - Correlation of high Resolution Remote Sensing Data with Field Samples. Environmental Modeling & Assessment, 12(4), 315-328.

Waser, L.T., Baltsavias, E., Ecker, K., Eisenbeiss, H., Ginzler, C., Küchler, M., Thee, P., & and Zhang, L. (2008). High-resolution digital surface models (DSM) for modeling fractional shrub/tree cover in a mire environment. International Journal of Remote Sensing, 29(5), 1261 – 1276.

Waser, L.T., Baltsavias, E., Ecker, K., Eisenbeiss, H., Feldmeyer-Christe, E., Ginzler, C., Küchler, M., Thee, P. and Zhang, L. (2008). Assessing changes of forest area and shrub encroachment in a mire ecosystem using digital surface models and CIR-aerial images. Remote Sensing of Environment 112(5): 1956-1968.

Waser, L.T., Klonus, S., Ehlers, M., Küchler, M., and Jung, A., 2010. Potential of Digital Sensors for Land Cover and Tree Species Classifications - A Case Study in the Framework of the DGPF-Project. Photogrammetrie, Fernerkundung und Geo-information, Vol. 10 (2), pp. 132- 141.

Waser, L.T., Ginzler, C.; Kuechler, M.; Baltsavias, E.; Hurni, L., 2011. Semi-automatic classification of tree species in different forest ecosystems by spectral and geometric variables derived from Airborne Digital Sensor (ADS40) and RC30 data. Remote Sensing of Environment 115: 76-85.

P 18.1

Recent efforts on APEX Calibration and Validation

Petra D'Odorico, Andreas Hueni, Michael Jehle, Michael Schaepman

Remote Sensing Laboratories, Dept. of Geography, University of Zurich, Winterthurerstrasse 190, 8057 Zurich

The generation of high-accuracy Earth System Science prodcuts based on remote sensing system relies on accurate system and data calibration, which ties data to international, physical standards.

The imaging spectrometer APEX (Airborne Prism Experiment) operates in the visible and near infrared region of the electromagnetic spectrum and has been designed to acquire Earth System related measurements.

In order to achive the required accuracy, a detailed characterisation and calibration of the instrument is carried out on a regular basis on the Calbration Home Base (CHB) at DLR Oberpfaffenhofen.

The provision of calibrated data requires a stable and quality controlled data pool storing the vast amount of CHB data upon which calibration routines can be applied in a transparent, operational and repeatable manner.

The APEX Calibration Information System (APEX CAL IS) has been developed for the above reasons. It provides the means for monitoring the stability of the instrument over time. Comparison over time allows continuous quality checks during calibration at the CHB, reducing the risk of acquiring data with wrong or suboptimal CHB or instrument settings.

APEX takes calibration one step further by including in-flight monitoring of instrument performances. Differences between the laboratory and the airborne environment, in terms of environmental conditions and operational interfaces, can thus be taken into account during calibration. The instrument features onboard characterization equipment, such as an internal light source and spectral filters, known as the In-Flight Characterization (IFC) facility. Onboard characterization measurements are regularly acquired at closed shutter before and after every target, as well as on-ground. Performance correction coefficients can be derived from these measurements and applied to the imaging data acquired in flight. The APEX all-round calibration concept allows delivering physically meaningful data to the users and provides a data pool for calibration, simulation and validation of other optical airborne and spaceborne instruments.

P 18.2

Short-term variability within long-term trends in global vegetation activity

Rogier de Jong [1,2], Jan Verbesselt[1], Michael E. Schaepman [3], Sytze de Bruin[1]

[1] *Laboratory of Geo-Information Science and Remote Sensing, Wageningen University, The Netherlands*
[2] *ISRIC – World Soil Information, Wageningen, The Netherlands*
[3] *Remote Sensing Laboratories, University of Zurich, Switzerland*

Continuous global time series of vegetation indices (VIs), which are available since early 1980s, are of great value to detect changes in vegetation activity at large spatial scales. Station-based phenological observations (e.g. Menzel et al., 2006) and these VI time series (e.g. Zhou et al., 2001) have shown evidence for greening and browning trends during the past decades in several regions in the world. These trends in vegetation activity may, over time, consist of an alternating sequence of greening and/or browning periods (e.g. Angert et al., 2005). Most change detection methods, however, assume a fixed change trajectory – defined by the start and end of the time series – and a linear or monotonic trend. We applied a change detection method, which detects abrupt changes within the time series in a data-driven manner, i.e. without prior knowledge on location or timing. This Breaks For Additive Season and Trend (BFAST) approach showed that large parts of the world were subjected to trend changes since the start of the satellite record in 1981. Many of these changes were found around large-scale natural influences like the Mt Pinatubo eruption in 1991 and the strong 1997/98 El Niño event, especially in grassland and shrubs. Shifts from greening to browning (or vice versa) occurred in 15% of the global land surface, which demonstrates the importance of accounting for trend breaks when analyzing long-term NDVI time series.

REFERENCES:
Angert, A., Biraud, S., Bonfils, C., et al. (2005). DOI: 10.1073/pnas.0501647102
Menzel, A., Sparks, T.H., Estrella, N., et al. (2006). DOI: 10.1111/j.1365-2486.2006.01193.x
Zhou, L., Tucker, C.J., Kaufmann, R.K., et al. (2001). DOI: 10.1029/2000JD000115

P 18.3

Visual Localization Recognition and Photo-to-Terrain-Alignment in Mountainous Areas

Olivier Saurer and Georges Baatz and Kevin Köser and Marc Pollefeys

Computer Vision and Geometry Group, ETH Zürich, CH-8092 Zürich

In this work we address the problem of registering terrestrial images to a digital elevation model, by estimating the six degree of freedom (rotation and translation) of the camera pose. What makes this problem lot harder than registration in urban environments is the different appearance of the mountains due to time of day and time of year. Relief-like structures and cracks cause very different image patterns depending on the illumination (shadows) and the appearance of the mountains varies a lot according to the amount of snow, the snow line, glaciers borders and vegetation which vary within and between seasons.

More stable features seem to be the contours and also other lines on the mountains. Although a large fraction of the line segments will not reappear under different conditions (time of day, shadows, time of year, different perspective), initial experiments show promising results. In particular, the skyline is virtually invariant (ignoring snow piles in winters and small changes by trees on the ridges) and often very discriminative even within 1000km^2.

To extract skylines of the model, we extract panoramic images from a 30km x 30km area with a 100m grid resolution, see figure[1]. The panoramas are represented as cubemaps, from which the contours can efficiently be extracted and represented on the unit sphere. In a similar way contours are extracted from a terrestrial image. The registration is achieved by comparing the contour lines of the panoramic and the terrestrial image.

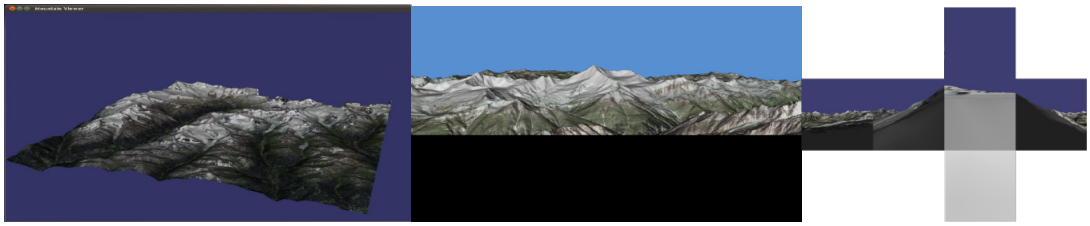

Figure 1: Elevation model of 30km x 30km area size, textured with orthographic aerial images (left). The model resolution is 2 m^2 per grid point. Close-up view (middle). Right, cubemap representation of a 360 degree view. Top and bottom face of the cube (dark and light blue squares) represent the sky and the ground respectively.

We evaluate the algorithm by exhaustively searching for the best matching image on a 30 km x 30 km grid, sampled at a distance of 100m. The error term evaluated for each image pair, is visualized in figure [2] left. Figure [2] right, shows the best matching skyline overlaid onto the terrestrial image. For the first set of test images this method shows an optimum near the true position (light green), meaning that the registration could be solved reasonably well. In the future we plan to replace the computationally costly exhaustive search by efficient indexing methods known from web/test search.

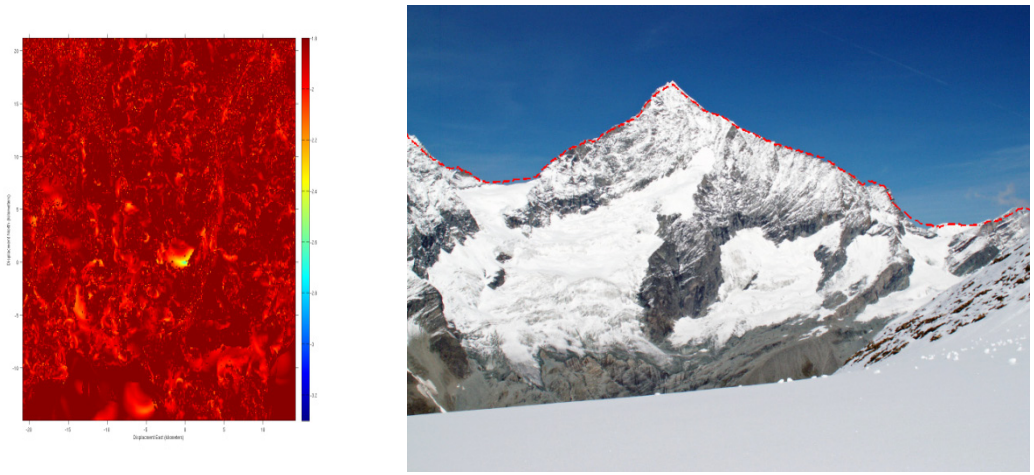

Figure 2: Left, evaluation of the error term over a grid size of 30km x 30km sampled at a distance of 100m. The optimal position (light green) is close to the true position. Right, overlay of the best matching synthetic skyline with the terrestrial image.

BIBLIOGRAPHY

1. *Vision-Based Localization.* **Thompson, William B., et al.** s.l. : ARPA, Morgan Kaufmann, 1993.
2. *Position Estimation from Outdoor Visual Landmarks for Teleoperation of Lunar Rovers.* **Cozman, Fabio and Krotkov, Eric.** s.l. : Proc. Third IEEE Workshop on Applications of Computer Vision, 96. pp. 156--161.
3. *Estimating Camera Position and Orientation from Geographical Map and Mountain Image.* **Jr, Prospero C. Naval, et al.** [ed.] Society of Instrument and Control Engineers 38th Research Meeting of the Pattern Sensing Group. 1997. pp. 9--16.
4. *Groups of Adjacent Contour Segments for Object Detection.* **Ferrari, V., et al.** s.l. : IEEE Computer Society, 2008. Vol. IEEE Transactions on Pattern Analysis and Machine Intelligence, pp. 36-51.
5. *Alignment by Maximization of Mutual Information.* **Viola, Paul, Wells, III and M., William.** s.l. : Kluwer Academic Publishers, 1997. pp. 137--154.
6. *Automatic Photo-to-Terrain Alignment for the Annotation of Mountain Pictures.* **Baboud, Lionel, et al.** Colorado Springs, USA : IEEE, 2011.
7. **VirtualPlanetBuilder.** s.l. : openscenegraph.org.
8. *Object Recognition from Local Scale-Invariant Features.* **Lowe, D.G.** [ed.] ICCV99. 1999.

P 18.4

Long-term geolocation accuracy of TerraSAR-X high-resolution spotlight products

Schubert Adrian[1], Small David[1], Jehle Michael[1] & Meier Erich[1]

[1]*Remote Sensing Laboratories, University of Zurich, CH-8057 Zurich (adrian.schubert@geo.uzh.ch)*

A SAR sensor with high geolocation accuracy greatly simplifies the task of combining multiple data takes with one another, not only simplifying their inter-comparison, but also dramatically speeding up applications such as near-real-time disaster mapping. Accurate geolocation also permits multiple image products to be quickly combined or layered with other data sources such as digital elevation models, cadastral maps, vegetation maps, forest maps, etc.

The extremely high orbital and product geolocation accuracy of TerraSAR-X (TSX) has been established in past validation studies conducted by various research groups (Eineder et al. 2011, Schubert et al. 2010, 2011). In particular the stripmap and high-resolution spotlight (HS) products, with their sample intervals ranging from 0.5 m to 2 m, offer one of the highest geometric resolutions currently available to the scientific community. However, achieving the highest-possible accura-

cy from these products requires correcting for at least two perturbing factors: (a) atmospheric path delay due to refraction, and (b) solid Earth tides (SETs). In this study, ground measurements were surveyed using differential GPS (DGPS). Because of differences between the local and global geodetic reference frames caused by continental plate tectonics, a plate-drift model was also incorporated into our location estimates.

A time series of images spanning 16 months was obtained over a fixed test site in the west of Switzerland (*Torny-le-Grand*), making it possible to validate both an atmospheric refraction and a SET model, while at the same time establishing the instrument's long-term stability. These related goals were achieved by placing trihedral corner reflectors (CRs, two shown in Figure 1) at the test site, and estimating their phase centers with centimeter-level accuracy using DGPS. Oriented in pairs towards a given satellite track, the CRs could be seen as extremely bright points in the images, providing a geometric reference set.

SAR images from the TSX HS mode were obtained in alternating ascending and descending orbit configurations. The highest-resolution products were selected to enable determination of their positions at the best possible precision. Based on the delivered product annotations, the CR image positions were predicted, and these predictions were compared to the actual measured image positions both before and after compensation for atmospheric refraction and systematic solid-Earth deviations.

The study was able to demonstrate that when the delivered product timing annotations are corrected for path delay and SETs using simple models, the TerraSAR-X products deliver unprecedented geolocation accuracy. Furthermore, this accuracy was maintained for the duration of the 16-month test period.

Figure 1. Trihedral corner reflectors in *Torny-le-Grand* facing TerraSAR-X's descending orbit.

REFERENCES

Eineder, M., Minet C., Steigenberger P., Cong X. & Fritz T. 2011: Imaging Geodesy – Toward centimeter-level ranging accuracy with TerraSAR-X, IEEE Transactions on Geoscience and Remote Sensing, 49(2), 661–671.

Schubert, A., Jehle, M., Small, D. & Meier, E. 2010: Influence of Atmospheric Path Delay on the Absolute Geolocation Accuracy of TerraSAR-X High-Resolution Products. IEEE Transactions on Geoscience and Remote Sensing, 48(2), 751–758.

Schubert, A., Jehle, M., Small, D. & Meier, E. 2011: Mitigation of atmospheric perturbations and solid-Earth movements in a TerraSAR-X time-series. Journal of Geodesy (cond. accepted).

P 18.5

Data fusion methods of LiDAR and spectroscopy data for the derivation of forest biochemical and biophysical variables – a review

Hossein Torabzadeh, Felix Morsdorf, Michael E. Schaepman

Remote Sensing Laboratories, Department of Geography, University of Zurich, Winterthurerstr. 190, CH-8507 Zurich, Switzerland (hossein.torabzadeh@geo.uzh.ch)

Nowadays, multi-source data fusion is an important method to improve our understanding of forest functioning. Due to the available diversity of data sources in remote sensing, fusion methods play a critical role in estimating forest parameters. LiDAR (Light Detection and Ranging) systems and imaging spectrometers in particular have capabilities, which should ultimately provide reliable information on the state of forest ecosystem. LiDAR data can provide structural forest parameters such as tree height and fractional cover, while other parameters (e.g. true LAI or fAPAR) can only be determined accurately using complementing data sources. Imaging spectrometer data are used to assess biochemical variables of vegetation canopies, but their retrieval quality is strongly dependent on the structural heterogeneity of a forest. Like in any other data fusion method, choosing the appropriate method is a critical issue allowing the full exploitation of their complementarities. We review and analyze fusion approaches for these two acquisition methods. Structurally, we divide approaches into levels (fusion at data or product level) and methods (physically vs. empirical methods), and discuss theses approaches in detail.

P 18.6

Ross-Li BRDF correction of airborne imaging spectroscopy data for improved continuous field map generation in the Swiss National Park

Weyermann Joerg[1], Damm Alexander[1], Kneubühler Mathias[1] & Schaepman Michael[1]

[1]*Remote Sensing Laboratories, Geographisches Institut, Universität Zürich, Winterthurerstr. 190, 8057 Zürich (joerg.weyermann@geo.uzh.ch)*

Uncertainty in quantitative Imaging Spectroscopy (IS) data analysis can be introduced by a number of factors, e.g. sensor calibration, data pre-processing and atmospheric correction, anisotropy of the atmosphere or ground reflectance anisotropy issued by view angle changes over the across-track field of view (FOV). While much effort is put into sensor calibration and atmospheric correction, and anisotropy of the atmosphere plays a role only at very large off- nadir view angles and turbid atmosphere, ground reflectance anisotropy was found to cause significant uncertainties both on the hemispherical-directional reflectance factor (HDRF) data and on product level. While difficult especially for airborne IS data where no information on the angular reflectance behavior of a surface can be derived from the data, the normalization of HDRF anisotropy effects is absolutely critical for the reliability of a data products derived from the data. Advanced products like continuous field maps of surface parameters of interest (e.g. columnar surface water content) can only be generated with sufficient accuracy when the HDRF data were previously corrected for these effects. For operational correction, empirical or semi-empirical models can be used, which rely on a meaningful aggregation of data in order to estimate the surface BRDF shape over the FOV to generate a correction function. The semi- empirical Ross-Li model is well known and can also be used for airborne data (Weyermann et al. 2011). The model assumes that changes in the HDRF over the FOV are caused by ground HDRF anisotropy exclusively, which is only given when different factors causing illumination differences can be excluded. Solar angle changes can be disregarded in most cases, since no significant impact occurs during the acquisition of a single flight line. Topography, however, causes a spatial pattern that biases the estimation of ground HDRF and possibly overrides or fully hides the effect of the target anisotropy. The Ross-Li model can be applied also in case of mountainous terrain, but information on a pixel›s individual configuration regarding illumination and observation geometry must be taken into account.

This contribution reports on current achievements in BRDF correction in a 2010 APEX dataset acquired over the Swiss National Park (SNP). For Ross-Li parameterization, slope and aspect information is derived from a 25m digital elevation model (Swisstopo DHM25) in order to account for the topography- dependent relative illumination and observation geometry.

Results are evaluated with continuous field maps of various surface parameters and biochemical products calculated by inversion of the PROSPECT/SAIL radiative transfer model.

REFERENCES

Weyermann, J., Damm, A., Kneubühler, M. & Schaepman, M. 2011: Assessing the effect of BRDF on Imaging Spectroscopy data and products using the Ross- Li correction method. – in preparation.

P 18.7

Influence of gap fraction on coniferous needle optical properties measurements

Yáñez-Rausell Lucía[1,2], Malenovský Zbynek[2], Schaepman Michael[2]

[1]*Centre for Geo-Information, Wageningen University, Droevendaalsesteeg 3/PO Box 47, 6700 AA Wageningen, The Netherlands (lucia.yanezrausell@geo.uzh.ch)*

[2] *RSL, Department of Geography, Univ. of Zurich, Winterthurerstrasse 190, CH-8057 Zurich, Switzerland*

Optical properties (OPs) of non-flat narrow leaves, i.e. coniferous needles, are extensively used by the remote sensing community, e.g. for calibration and validation of radiative transfer models at both leaf and canopy levels. Measurement of such small elements is, however, a technical challenge with a very little knowledge about related errors. Consequently two situations appear among the users of OPs: 1) the lack of such measurements forces them to make assumptions with a potentially negative impact on the interpretation of remote sensing data of coniferous forests (e.g. in radiative transfer modelling, needle transmittance is often assumed to be zero, or needle reflectance and transmittance are assumed to be equal); or 2) the used available datasets are of unknown reliability. This demonstrates a need for a robust, efficient and systematic measuring technique of narrow-leaf OPs.

Compared to the broad leaves, measurement of reflectance (R) and transmittance (T) of narrow leaves require adapting the conventional techniques (i.e. coupling a spectroradiometer to an integrating sphere) to a sample size smaller than the area illuminated by the incident light beam. Reduction of the illuminated area to the dimensions of one narrow leaf would result in a very low signal-to-noise performance. An alternative solution is to measure the signal from several needles simultaneously mounted next to each other in a carrier, and to correct such measurement for the portion of photons passing through the air gaps (gap fraction of the illuminated area – GF). The objective of this paper is to estimate an error budget of this technique by analysing errors originating from: 1) use of the carrier, 2) gap fraction estimation via digital image processing, and 3) multiple scattering caused by the non-flat nature of the needle leaves. To achieve this we measured OPs from an optically stable silicon material, which was cut in 1 mm thick strips to simulate needle shaped leaves. We build on the results presented by Mesarch et al. (1999) in which this technique was applied only on flat film paper, and we investigated the influence of the non-flat objects (needle leaves) on accuracy of the measurements. Computed R and T for different tested settings (i.e. carrier combinations, image processing settings, and distances between measured needles) were analysed to point out the best configurations and to estimate errors introduced by this technique.

REFERENCES

Mesarch, M.A., Walter-Shea, E.A., Asner, G.P., Middleton, E.M. & Chan, S.S. 1999: A revised measurement methodology for conifer needles spectral optical properties: evaluating the influence of gaps between elements. Remote Sensing of Environment, 68, 177–192.

P 20.8

Towards spectroscopic modelling of composite mineralogy

V.L. Mulder[a,*], S. de Bruin[a], M.E. Schaepman [a,b]

[a] *Laboratory of Geo-Information Science and Remote sensing, Wageningen University, Droevendaalsesteeg 3, P.O. Box 47, 6700 AA Wageningen, The Netherlands*

[b] *Remote Sensing Laboratories, University of Zürich, Winterthurerstrasse 190, 8057 Zürich, Switzerland*

[*] *Titia.mulder@wur.nl*

Soil mineralogy is an important indicator for soil fertility, soil formation and suitability. However, the determination of mineralogy by powder diffraction is costly and labour-intensive. Therefore, soil scientist do have need for an efficient method to determine the mineral composition of the soil. VNIR spectroscopy has proven to be an efficient method for the determination of various soil properties. Currently, single soil minerals can be determined with absorption feature analysis or spectral unmixing. For the prediction of multiple minerals the determination becomes more complex since the minerals, but also vegetation components, do have similar absorption features which complicates unmixing. With unconstrained spectral mixture analysis based on a single model, the composite soil mineralogy cannot be determined. The use of multiple models does improve the unmixing but the dominant minerals with spectral similarity are in most cases not discriminated. Also, quantification of the different minerals present in the composite is not feasible. However, the unmixing does provide information on the type of minerals present in the sample. The results were successfully related to lithological indices derived from thermal infrared ASTER satellite data. The results demonstrate that the mineral composition is difficult to relate to the spectral data using a simple forward model approach. Therefore, we suggest to develop a linear spectral trend model which is capable of predicting the main composite mineralogy based on VNIR spectroscopy.